

A METHODOLOGY OF UNSTEADY INVESTIGATIONS OF HELICOPTER AIRFOILS

Andrzej Krzysiak, Paweł Ruchała
Institute of Aviation

Summary

The paper describes a methodology of unsteady experimental investigations of helicopter airfoils. It has been implemented during tests of helicopter airfoil, carried out in Aerodynamics Department of Institute of Aviation for PZL-Świdnik and Ministry of Science and Higher Education (MNiSW – Ministerstwo Nauki i Szkolnictwa Wyższego) as a part of grant: “Development and deployment of new generation of design, technological and material solutions for main rotor and airframe elements of PZL W-3A Sokół helicopter”.

The tests have aimed to modeling (in the wind tunnel) the dynamic stall phenomena incidence, which may appear on main rotor blades during forward flight. It causes a strong vibration of blades, thus defining a considerable limit of helicopters' performance.

The dynamic stall phenomena is caused by fast angle of attack transition, which appears during forward flight. A similar transition on tested model was evoked by its oscillations with requested amplitude and frequency. The mechanism causing the oscillations of model and the measurement equipment have been described further.

The discussed methodology covers pressure distribution measurements, basing on measurement of local static pressure on the surface of respectively adapted model. Because the measurements of pressure are not simultaneous, the pressure coefficient distribution (as a function of time and angle of attack) has been approximated using Fourier series. The coefficients of lift and pitching moment have been calculated as a result of integration the pressure coefficient distribution. An algorithm of calculation has been described also.

Acknowledgements

The investigation has been carried out as a part of the grant: “Development and deployment of new generation of design, technological and material solutions for main rotor and airframe elements of PZL W-3A Sokół helicopter” („Opracowanie i wdrożenie nowej generacji rozwiązań konstrukcyjnych, technologicznych i materiałowych dla wirnika nośnego i elementów płatowca śmigłowca PZL W-3A Sokół”) for Ministry of Science and Higher Education (Ministerstwo Nauki i Szkolnictwa Wyższego) and PZL – Świdnik.

Notation:

a_i – ($i=0\dots N$) the coefficients of function approximating $C_p(t)$ and $\alpha(t)$ function

b_i – ($i=1\dots N$) the coefficients of function approximating $C_p(t)$ and $\alpha(t)$ function

c – airfoil chord [mm]

C_0 – the coefficient of ESP-16HD sensor's characteristic [psi]

C_1 – the coefficient of ESP-16HD sensor's characteristic [psi/mV]

C_2 – the coefficient of ESP-16HD sensor's characteristic [psi/mV²]

C_3 – the coefficient of ESP-16HD sensor's characteristic [psi/mV³]

C_4 – the coefficient of ESP-16HD sensor's characteristic [psi/mV⁴]

C_m – pitching moment coefficient (about quarter-chord point) [-]

$C_{m_{min}}$ – minimal pitching moment coefficient (about quarter-chord point) [-]

C_N – normal force coefficient [-]

C_p – pressure coefficient [-]

C_T – tangential force coefficient [-]

C_L – lift coefficient [-]

$C_{L_{max}}$ – maximal lift coefficient [-]

D – index of angular location sensor division [-]

D_0 – index of angular location sensor division related to $\alpha=0$ [-]

f – frequency of oscillation [Hz]

Ma – Mach number [-]

N – number of components of Fourier series approximating $C_p(t)$ and $\alpha(t)$ function [-]

p – local static pressure [kPa]

p_0 – total pressure of freestream [kPa]

p_S – static pressure of freestream [kPa]

q – dynamic pressure of freestream [kPa]

R^* – radial coordinate of blade airfoil, normalized by blade radius [-]

Re – Reynolds number [-]

t – time [ms]

T – air temperature [K]

U – voltage registered by ESP-16HD sensor [mV]

U_T – voltage registered by temperature channel of ESP-16HD sensor [mV]

x - airfoil chord-wise coordinate [mm]

y - airfoil vertical coordinate [mm]

\bar{x} - x coordinate normalized by chord length [-]

- y coordinate normalized by chord length [-]

α - angle of attack [°]

α_{kr} - critical angle of attack [°]

α_B - base angle [°]

$\Delta\alpha$ - amplitude of oscillation [°]

$\Delta\alpha_{kr}$ - difference of critical angle of attack (in steady and unsteady conditions) [°]

ΔC_{Lmax} - difference of maximal lift coefficient (in steady and unsteady conditions) [-]

1. INTRODUCTION

Fast, periodic transitions of angle of attack appear very often on helicopter main rotor blades. They are caused by i.a. asymmetry of flow around rotor during forward flight. A transition of angle of attack, as a function of angle of blade rotation Ψ , is similar to sinusoid (in predominant part of rotor blade, especially in external part - for $R^* > 50\%$). It has been shown in fig. 1.

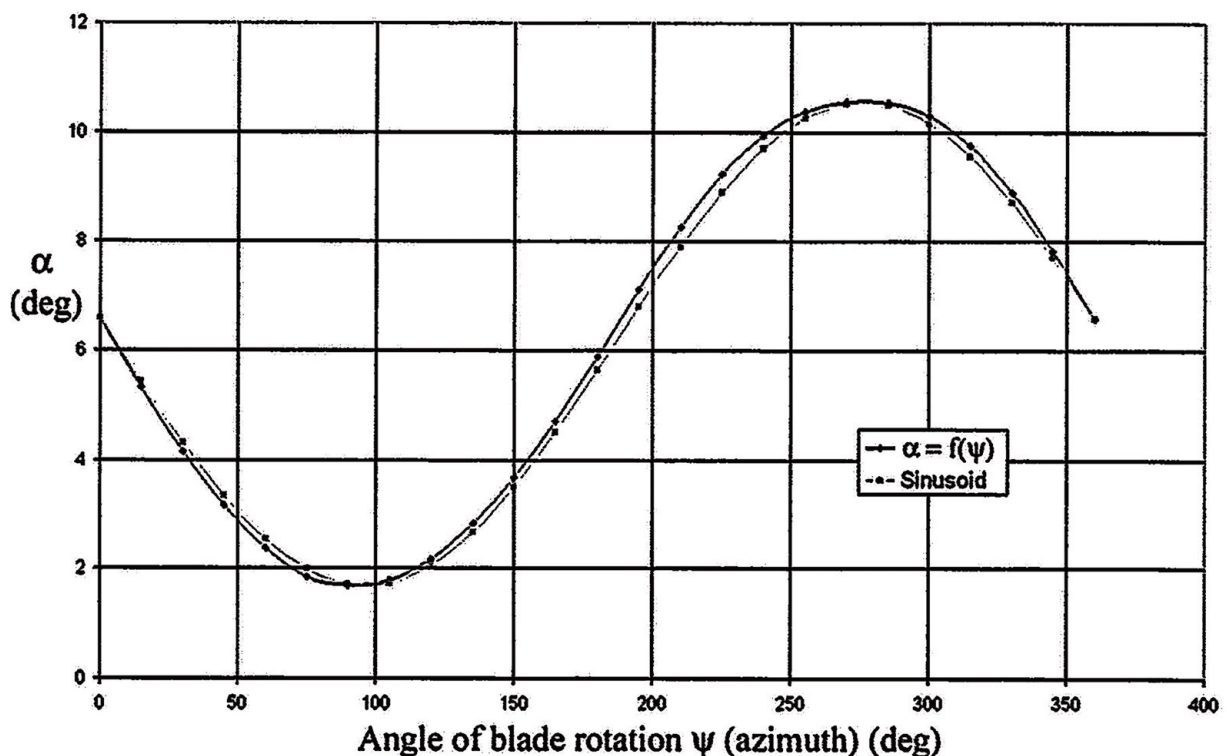


Fig. 1: A dependency of blade's angle of attack and angle of blade rotation, in comparison with the sinusoid ([3])

Because of fast transitions of blade's angle of attack, in some conditions there appears the so called "dynamic stall" phenomena. The range of its incidence has been shown in Fig. 2.

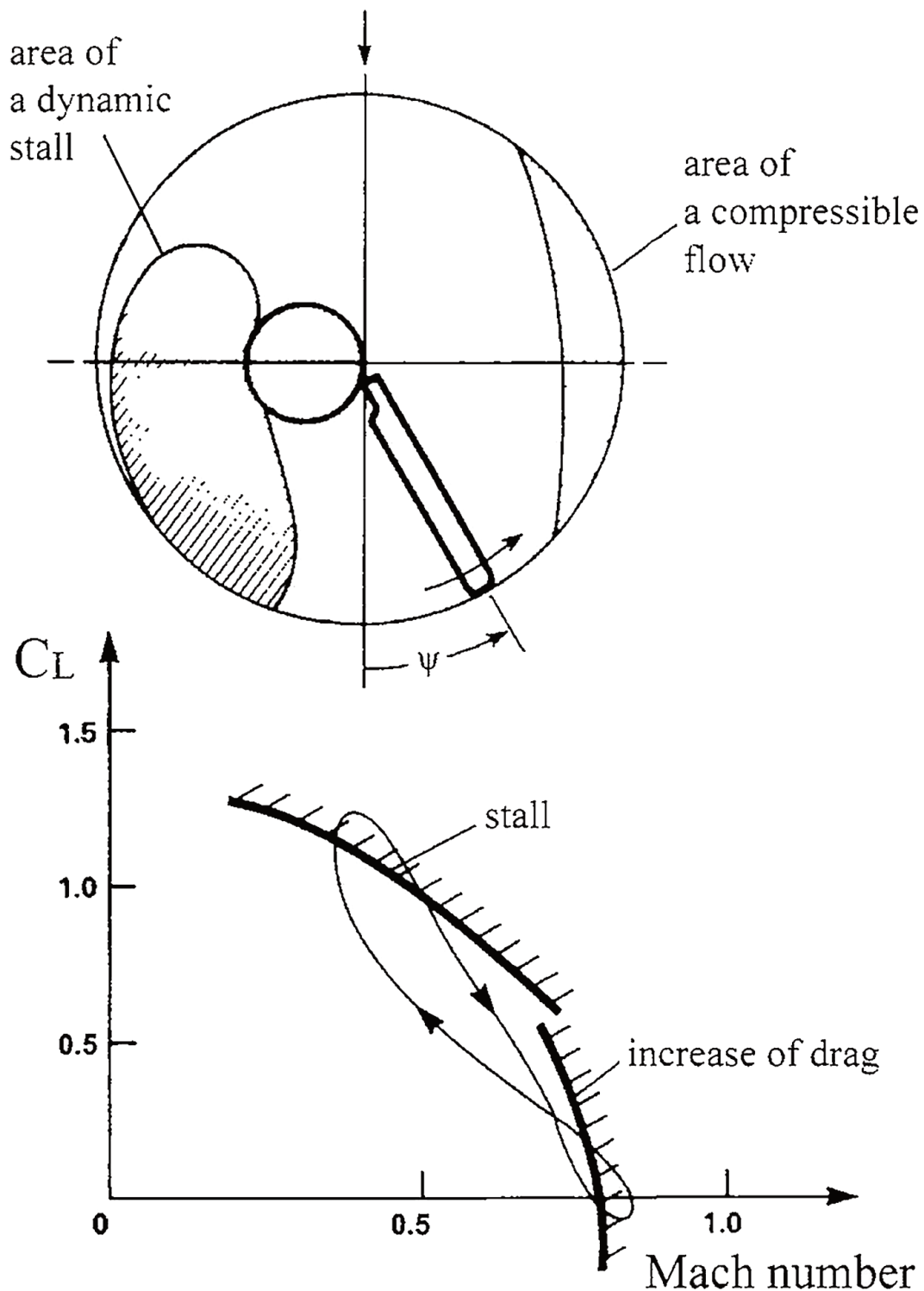


Fig. 2: The incidence of dynamic stall phenomena ([3])

The dynamic stall means, that flow separation on blade's upper surface has limited range, even after exceeding a critical (for static conditions) angle of attack. Because of it, much higher maximal lift coefficient than in static conditions can be achieved. The $dC_L/d\alpha$ derivative increases also. This effect is connected with a vortex created on blade's leading edge after exceeding a critical (for static conditions) angle of attack. The vortex moves toward trailing edge during angle of attack's increase, causing a step decrease of pitching moment.

The moment the vortex leaves blade's trailing edge, a lift force steeply decreases. Because the dynamic stall phenomena lasts very shortly, it may cause a rotor blade's vibrations, which constitute an important limitation of helicopters' performances [3].

2. TEST TECHNIQUE

2.1 N-3 Wind Tunnel

The dynamic stall phenomena, described above, has been sifted during investigations of helicopter main rotor airfoil. The investigation has been carried out on the model which was performing an oscillations with requested amplitude and frequency.

During the investigation a N-3 high-speed wind tunnel (shown in Fig. 3) has been used. It's a blow-down wind tunnel with partial re-circulation of the flow, which enables investigations in the subsonic, transonic and supersonic flow regimes. Available Mach number: $Ma = 0.2 \div 1.2$ (with continuous control of flow velocity), $Ma = 1.5$ or $Ma = 2.3$. Only when respective nozzle is mounted $Ma = 1.5$ and $Ma = 2.3$ are available.



Fig. 3: A part of N-3 high-speed wind tunnel (photo by A. Dziubiński, IoA)

N-3 wind tunnel has got a close test chamber, with 0.6x0.6 m square cross-section. Each side wall of test section is equipped with two double windows of 0.25 m diameter. Top and bottom walls are disposable. Solid and perforated walls may be mounted. During described tests the perforated walls have been used to decrease the walls' interference in the flow.

An exact description of N-3 wind tunnel and airfoils' test technique have been published in the paper [10]

2.2 TESTED MODEL

An investigated airfoil model is a rectangular wing, without aerodynamic and geometric twist. Its chord length equals 0.2 m and wing span –0.6 m. The wing span equals test chamber's width, so two-dimensional flow has been assumed (test chamber walls works as the endplates). The model, mounted in a wind tunnel test chamber, is shown in Fig. 4.

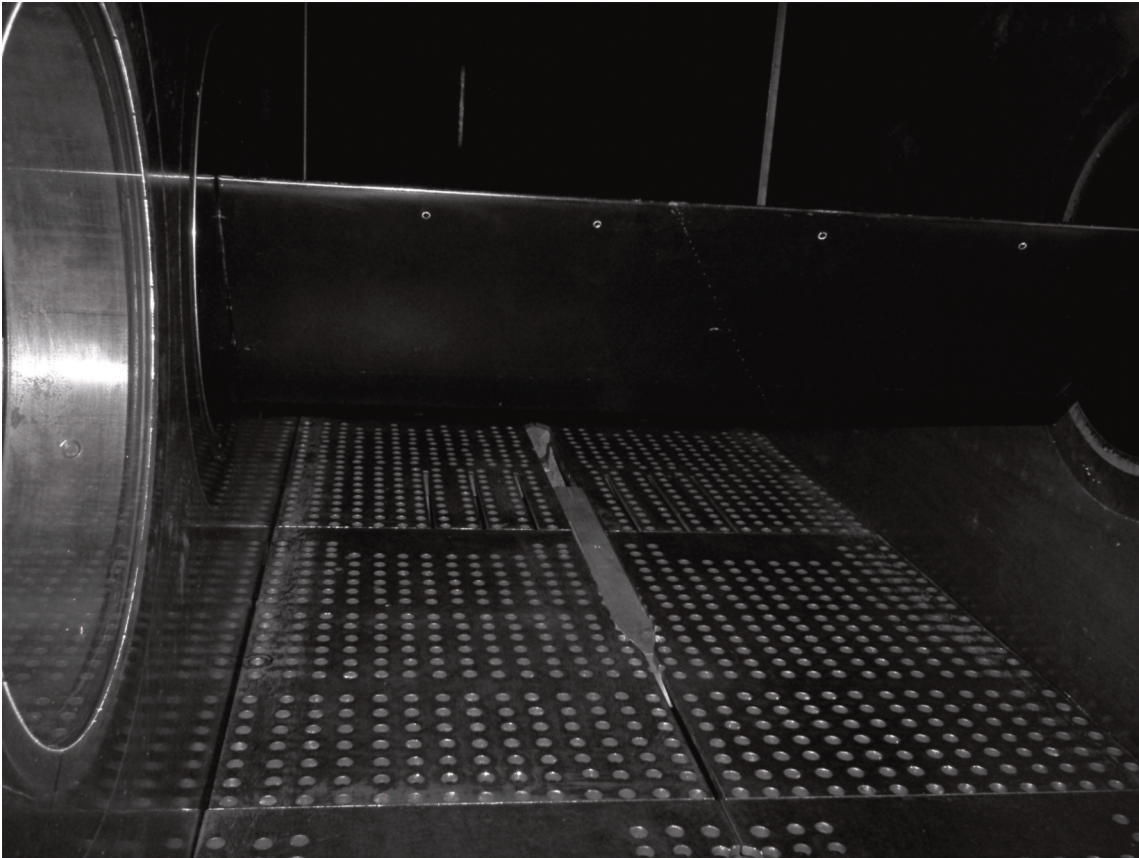


***Fig. 4. A model of investigated airfoil mounted in a wind tunnel test chamber
(photo by S. Podgródny, IoA)***

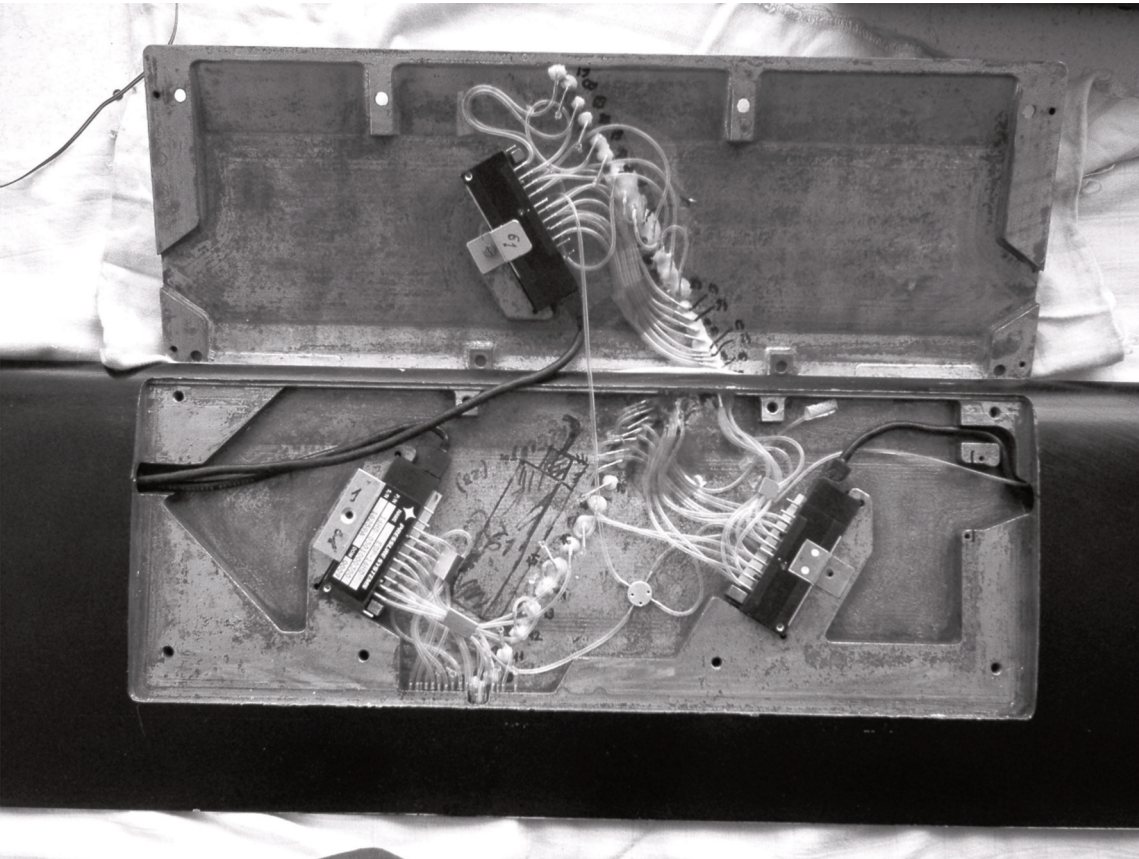


***Fig. 5: ESP-16HD pressure sensors mounted inside airfoil model
(photo by S. Podgródny, IoA)***

The tested model is all-metal and hollowed. Its upper surface part may be disassembled. It enabled mounting a pressure sensors inside the model, as shown in Fig. 5. Three 16-channel ESP-16HD by Pressure System Inc. pressure sensors have been used. The measured range equals ± 5 psi (for one of sensors, no. 59) or ± 10 psi (for two extant sensors, no. 60 and 61).

Sensors' inputs have been connected using thin pipes with appropriate pressure measurement points – i.e. 0.5 mm holes drilled on the model's surface. 69 holes have been drilled. Unfortunately, not all of them have been used, because only 48 sensors' channels were available. Arrangement of pressure measurement points is sketched in Fig. 6.

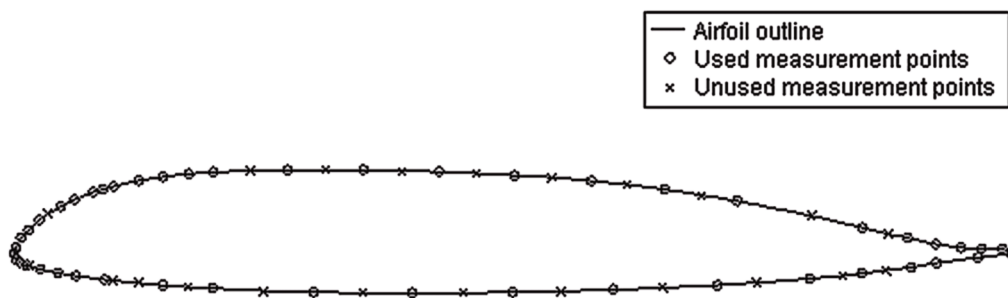


Fig. 6: Pressure measurement points arrangement

The airfoil's flow conditions were simulated in the wind tunnel by its oscillations around the so called „base angle” α_B . Thus the angle of attack is a sum of base angle and instantaneous value of oscillation angle:

$$\alpha \approx \alpha_B + \Delta\alpha \cdot \sin(2\pi \cdot f \cdot t)$$

Base angle was regulated by angle of attack mechanism, used in static investigations. This mechanism was joined with rod mechanism generating oscillations, which has been powered by electric engine. The whole device, shown in Fig. 7, has been connected with one side of the model's rotation axis. On the other side the angular location sensor ROC-412 by Heidenhain, registering the instantaneous value of angle of attack, has been mounted.

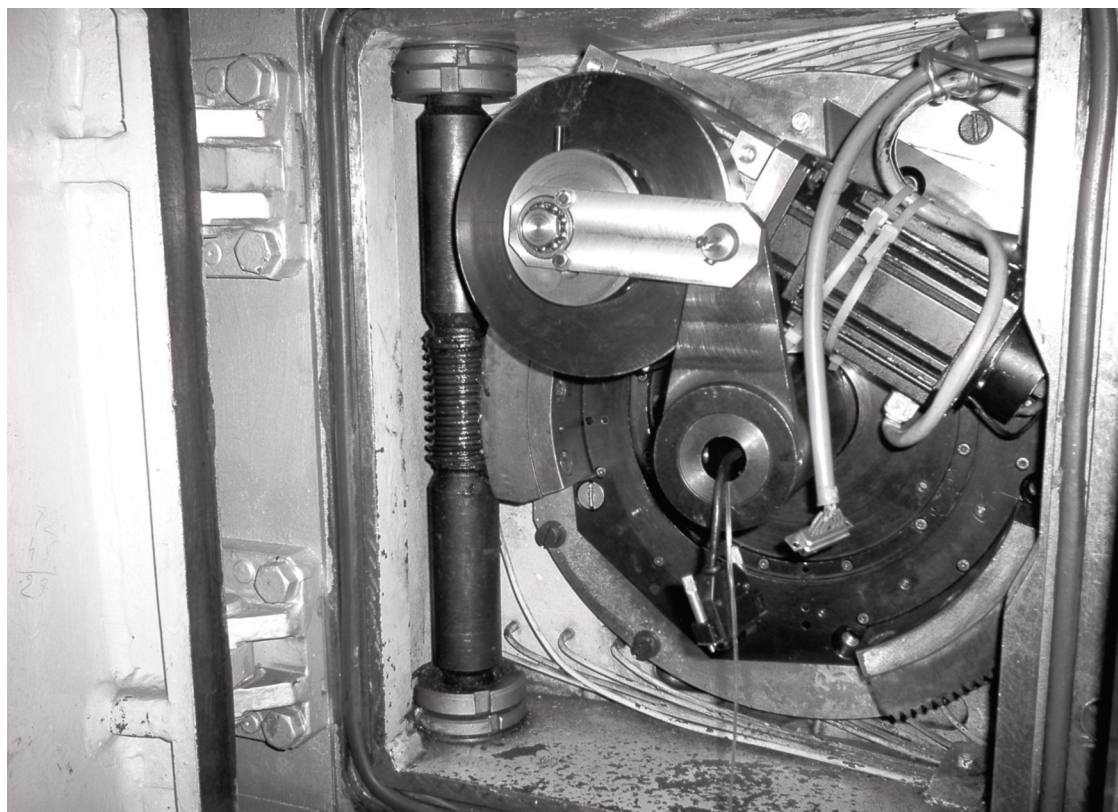


Fig. 7: A mechanism generating oscillations of the tested model (photo by S. Podgródny, IoA)

A device described above enables transition of oscillation frequency (up to 10 Hz) through the change of engine's angular velocity. Setting the oscillation amplitude ($\pm 5^\circ$ or $\pm 10^\circ$) was also possible by changing the point of rod's fixing to engine's fly-wheel. The whole device (with the angular location sensor) has been used also as a model's fixing in the test chamber – the mechanism and the angular location sensor have both been mounted in the windows in the side walls of the test chamber.

3. ALGORITHM OF CALCULATION PROCESS

The investigation results have been obtained in a four-stage process. The stages are as follows:

- Registration of measured values (during the test)
- Processing of every made run (test cycle), i.e. calculation of lift and pitching moment coefficients
- Analysis of results' correction
- Conclusions

For data registration (stage 1) the DYNAK program has been used. It handles the data acquisition devices connected with used sensors. The DYNAK program is a part of SPITA N-3/PC measurement system.

Parameters measured during the test are, among others:

- instantaneous value of static pressure on model's surface
- instantaneous value of angle of attack
- static and total pressure of freestream
- freestream temperature

The parameters listed above are saved by DYNAK program in various (both text and binary) files, which are a source for PdN-3 program, aimed at processing the runs' results.

PdN-3 program's calculations results are saved as a ASCII file. The program can make the graphs on its own or export data for other software – Grapher for example.

3.1. REGISTERED DATA

Usually one run contains several measurements for various base angles. During every measurement 256 data sets have been registered. Every set contains the information on instantaneous value of angle of attack (measured by ROC-412 angular location sensor) and on static pressure instantaneous values (measured by ESP-16HD pressure sensors).

In effect 256 instantaneous values of angle of attack and static pressure (for every measurement point) are available in whole measurement. It's not enough, however, for pressure distribution's calculating. Every instantaneous value is registered in different moment, because of measurement's duration.

Because of angle of attack's continuous transition, every instantaneous value of pressure corresponds with different angle of attack's value.

A sequence of data registration is shown in Fig. 8.

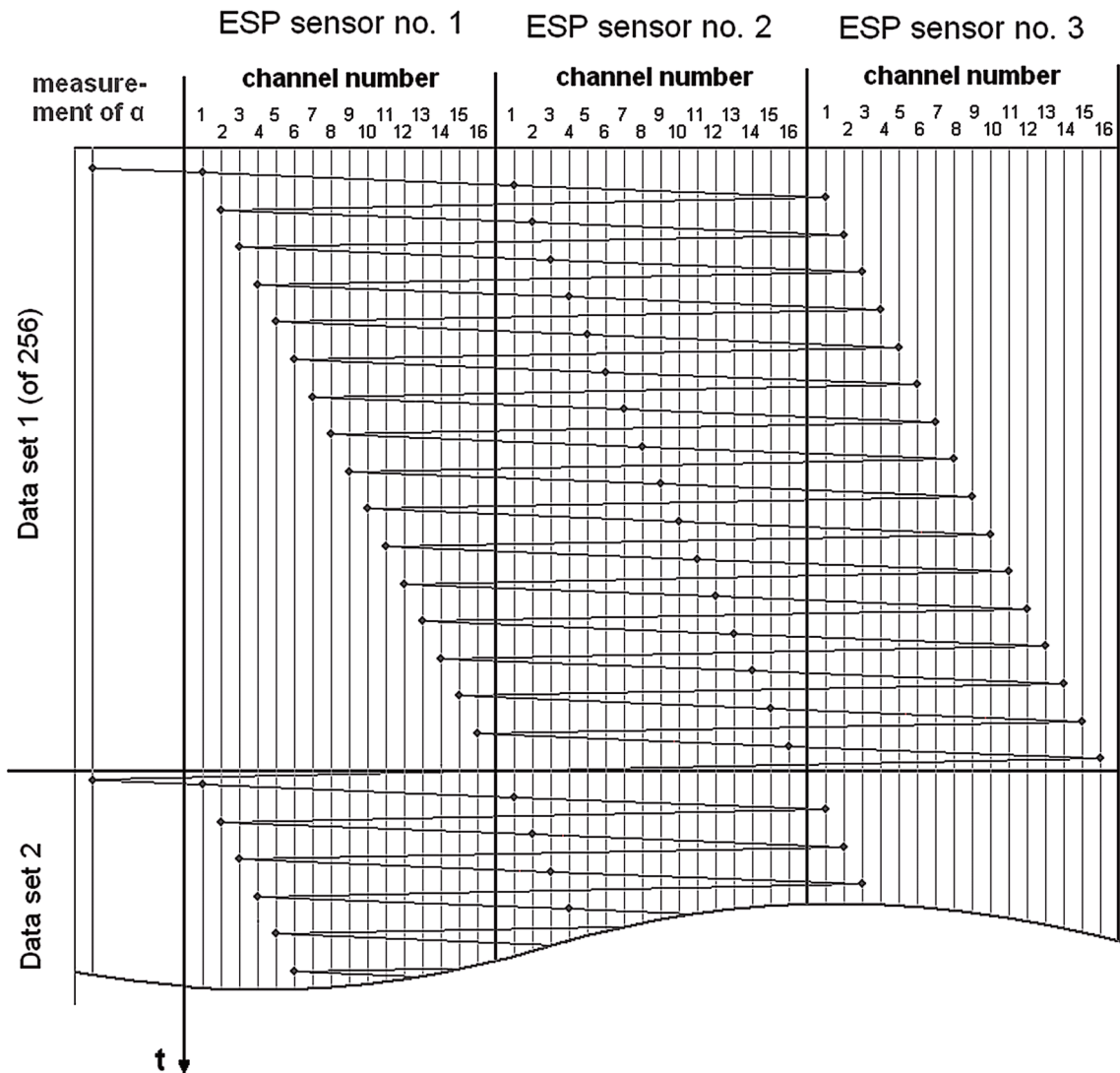


Fig. 8: A sequence of data registration

Except for data sets described above, during every run the following parameters of freestream have been registered: temperature, static pressure and total pressure. Temperature of every ESP-16HD sensor has been measured also.

3.2. PROCESSING

During processing stage the following actions have been taken:

1. Obtaining instantaneous value of angle of attack
2. Obtaining instantaneous value of static pressure on the model's surface
3. Obtaining instantaneous value of pressure coefficients C_p
4. Interpolation of $C_p(t)$ and $\alpha(t)$ – obtaining a pressure coefficient distribution for requested time
5. Integrating of the pressure coefficient distribution $C_p(x)$ – obtaining lift and pitching moment coefficient
6. Obtaining of Reynolds number

Because of lack of algorithm for interference correction during unsteady investigations, no corrections have been implemented.

Individual operations have been shortly described further:

3.2.1 CALCULATION OF INSTANTANEOUS VALUE OF ANGLE OF ATTACK

The ROC-412 angular location sensor is equipped with code-disc with 4095 divisions. Thus the information about angle of attack's value is an index of division, saved in a binary file. Basing on it, when number of division related to $\alpha=0$ is known, angle of attack may be calculated using equation:

$$\alpha = \alpha_B - (D - D_0) \cdot \frac{360}{4095} \text{ [deg]}$$

where:

α_B – base angle
 D – number of division registered during the test
 D_0 – number of division related to $\alpha=0$

Direction of positive angle of attack is opposite to the direction of division index's increase. Therefore in the equation above there appears the minus" sign.

3.2.2 CALCULATION OF INSTANTANEOUS VALUE OF STATIC PRESSURE ON MODEL'S SURFACE

Instantaneous value of static pressure have been calculated in 2 stages:

1. Calculation of voltage of respective ESP-16HD sensor channel, basing on binary data registered during the test
2. Calculation of pressure, basing on voltage obtained as above and on the channel characteristics:

$$p = C_0(U_T) + U \cdot C_1(U_T) + U^2 \cdot C_2(U_T) + U^3 \cdot C_3(U_T) + U^4 \cdot C_4(U_T)$$

$C_0...C_4$ coefficients are different for each channel, therefore it was needed to obtain 48 coefficients sets. Channel characteristics depend also on sensor's temperature, which is related to voltage of respective ESP-16HD sensor's temperature channel.

A dependency between temperature channel's voltage and $C_0...C_4$ coefficients has been obtained basing on producer's information. The results of calibrations made by Aerodynamic Division of Institute of Aviation have been used as well.

3.2.3 CALCULATION OF INSTANTANEOUS VALUE OF PRESSURE COEFFICIENT C_p

Instantaneous values of pressure coefficient have been obtained using equation:

$$C_p = \frac{p - p_s}{q}$$

where:

p – static pressure on a model's surface (in a respective measurement point)
 p_s – static pressure of freestream (measured by Solartron sensors, which are a part of SPITA N-3/PC system)
 q – dynamic pressure of freestream, obtained with equation:

$$q = 0.7 \rho p_s Ma^2$$

Ma – Mach number, obtained using equation:

$$Ma = \sqrt{5 \left[\left(\frac{p_0}{p_s} \right)^{\frac{2}{7}} - 1 \right]}$$

p_0 – total pressure of freestream (measured by Solartron sensors)

It is assumed that static, dynamic and total pressure of freestream and its Mach number are constant during the whole measurement.

3.2.4 AN INTERPOLATION OF CP(T) AND A(T) DEPENDENCIES

Basing on 256 instantaneous values of pressure coefficient C_p (for each measurement point) a $C_p(t)$ function has been approximated as a Fourier series:

$$C_p(t) = a_0 + \sum_{n=1}^N (a_n \cos(n\omega t) + b_n \sin(n\omega t))$$

where:

ω – frequency of model's oscillation

$a_0, a_1... a_N$ and $b_1... b_N$ – a coefficients of Fourier series, obtained with least squares method.

A dependency shown above enables calculation of instantaneous values of pressure coefficient C_p for requested time (identical for all measurement points). In the effect, pressure coefficient distribution, related to the requested time, may be obtained.

The instantaneous angle of attack values have been calculated in the same way.

It is clear, that $C_p(t)$ functions have been approximated as periodic functions, which period equals a period of model's oscillations. It's equivalent to the assumption that transitions of pressure distribution are the same during every period of oscillations.

This assumption is quite well fitted in practice. It has been shown in Fig. 9, which illustrates a dependency between pressure coefficient (in one of measurement points) and time, during the next periods of oscillation. The values obtained with Fourier series have been shown also.

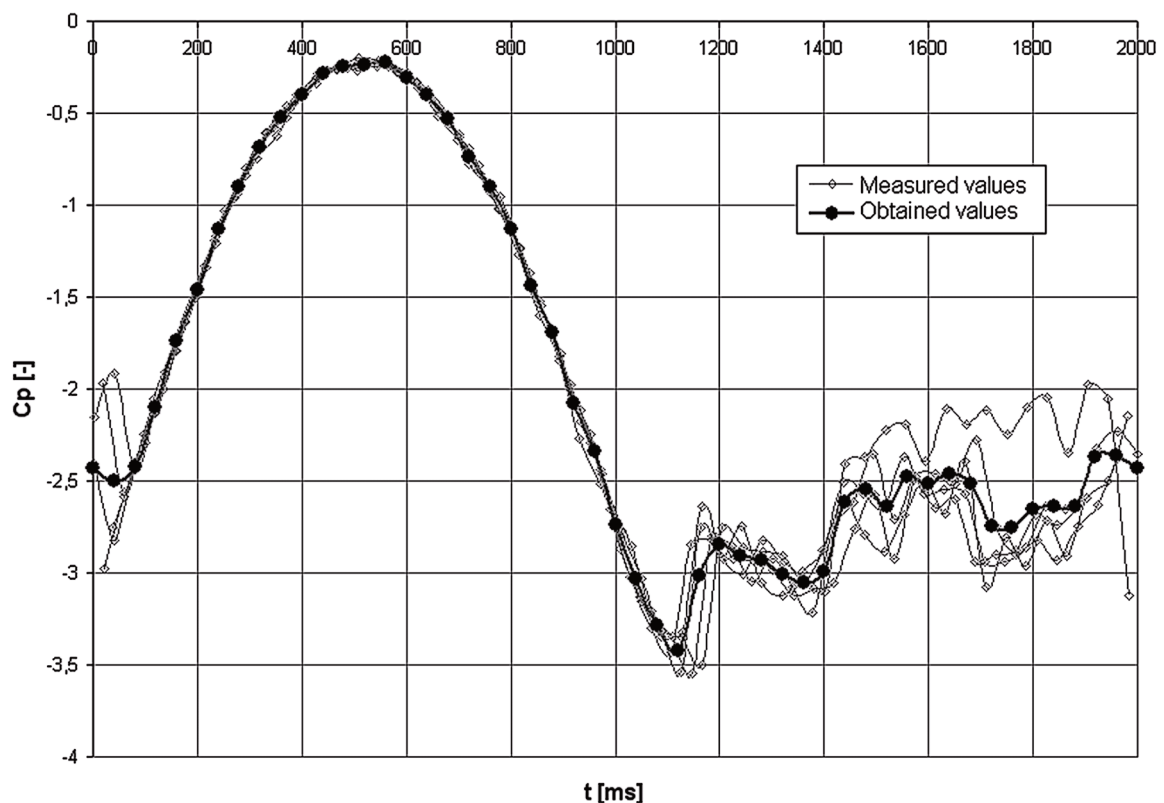


Fig. 9 : An example of $C_p(t)$ function, basing on approximated values and values measured during the next periods of oscillation

3.2.5 INTEGRATING OF PRESSURE COEFFICIENT DISTRIBUTION

An essence of pressure distribution measurement is calculation of aerodynamic force and moment coefficients basing on pressure coefficients obtained beforehand. By definition, the investigations of airfoil covers 2-D objects, thus only 2 force components (normal and tangential force) and 1 moment component (pitching moment) are needed to obtain.

Side force, roll moment and yaw moment are assumed zero. Lift coefficient is given by equation:

$$C_z = C_N \cdot \cos \alpha - C_T \cdot \sin \alpha$$

where normal force coefficient C_N and tangential force coefficient C_T have been calculated by pressure coefficient distribution integrating:

$$C_N = \int_{\text{airfoil outline}} C_p d\bar{x}$$

$$C_T = - \int_{\text{airfoil outline}} C_p d\bar{y}$$

where x and y - airfoil coordinates, normalized by the chord length.

Pitching moment coefficient is given by equation:

$$C_m = \int_{\text{airfoil outline}} C_p \cdot (\bar{x} - 0.25) d\bar{x} + \int_{\text{airfoil outline}} C_p \cdot \bar{y} d\bar{y}$$

3.2.6 CALCULATION OF REYNOLDS NUMBER

Reynolds number characterizes the conditions of measurement. This parameter is given by equation:

$$Re = 46.7 \cdot p_s \cdot Ma \cdot c \cdot \left(\frac{T}{1 + 0.2 \cdot Ma^2} + 124 \right) \cdot \frac{1}{\left(\frac{T}{1 + 0.2 \cdot Ma^2} \right)^2}$$

where:

p_s - static pressure [kPa]

Ma - Mach number [-]

c - chord length [m]

T - temperature [K]

The above equation has been derived using Reynolds number definition:

$$Re = \frac{\rho \cdot V \cdot c}{\mu}$$

and Sutherland's formula - a dependency between viscosity and temperature of air:

$$\mu = \mu_0 \frac{397}{T + 124} \cdot \left(\frac{T}{273} \right)^{3/2}$$

4. RESULTS AND CONCLUSION

The discussed investigations encompassed 18 runs. An oscillation amplitude equals $\Delta\alpha = \pm 5^\circ$ (in 16 runs) or $\Delta\alpha = \pm 10^\circ$ (in 2 extant runs). Mach number equals 0.3, 0.4, 0.5 or 0.75.

An oscillation frequency varied from $f = 0.3$ Hz to $f = 10$ Hz, and base angle - from $\alpha_B = -2^\circ$ to $\alpha_B = 14^\circ$.

An analysis of investigation results has demonstrated that:

A plot of lift coefficient C_L and angle of attack dependency have a loop shape. For lower values of angle of attack, where the flow separation on upper surface of the airfoil doesn't exist the hysteresis loop is relatively narrow. A variation between steady and unsteady investigations' results equals about $\Delta C_L = 0.05$ – both for increase and decrease of angle of attack.

The width of hysteresis loop increases for greater base angles, as shown in Fig. 10.

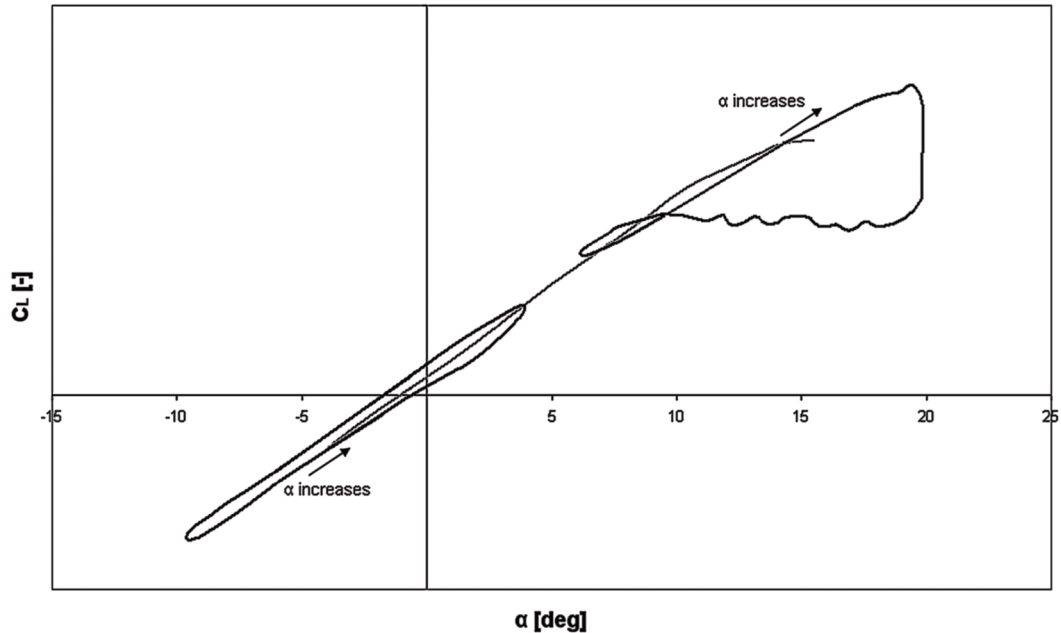


Fig. 10. An example of $C_L(\alpha)$ dependency, for base angle equal -2° and 14° and for static conditions

In most cases, during angle of attack increase, greater values of lift and pitching moment coefficients than during its decrease (but for the same instantaneous value of α angle) have been achieved.

A plot of pitching moment coefficient C_m and angle of attack dependency has a loop shape also, as shown in Fig. 11. For lower values of angle of attack the width of hysteresis loop is low as well.

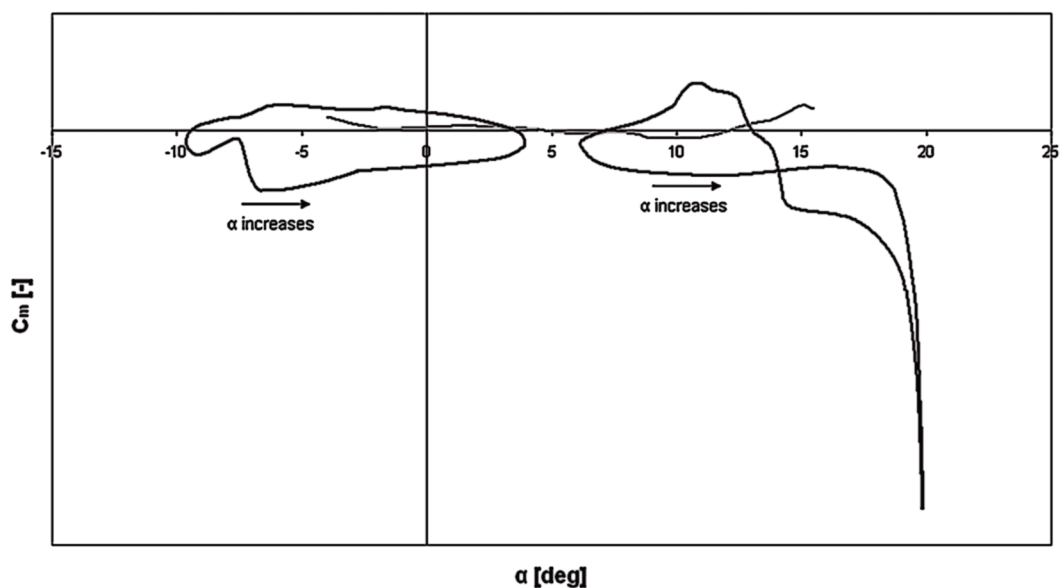


Fig. 11: An example of $C_m(\alpha)$ dependency, for base angle equal -2° and 14° and for static conditions

- An influence of Mach number and oscillation frequency on the width of hysteresis loop is very low.
- Maximal lift coefficient C_{Lmax} increases because of unsteady phenomena, and its increase exceeds $\Delta C_{Lmax} = 0.35$.
- Increase of oscillation frequency could cause an increase of critical angle of attack, up to $\Delta \alpha_{kr} = 4.5^\circ$ for investigated airfoil.
- For high values of angle of attack, above critical angle of attack approximately, a steep decrease of pitching moment coefficient, up to $Cm_{min} = -0.2$, has been observed.

LITERATURE

- [1] **Konopska D.**: „System pomiarowo – rejestracyjny SPITA N-3. Instrukcja Systemu Jakości ILot nr IS.04/LA”, 1997
- [2] **Krzysiak A.**: „Eksperymentalne badania charakterystyk aerodynamicznych profilu ILH-412 M-S w tunelu dużych prędkości N-3. Sprawozdanie wewn. ILot nr 23/BA1/08/P”, 2008
- [3] **Krzysiak A.**: „Experimental investigation of a dynamic stall on the oscillating NACA 0012 airfoil. Prace Instytutu Lotnictwa nr 187”, 2006.
- [4] **Krzysiak A., Żółtak J.**: „Eksperymentalne i numeryczne badania dynamicznego przeciągnięcia profili śmigłowcowych z uwzględnieniem wpływu efektu oblodzenia tych profili. Sprawozdanie wewn. ILot nr 51/BA/02/P”, 2002
- [5] **McCroskey W.J.** – „A critical assessment of wind tunnel results for the NACA-0012 airfoil”. NASA, 1987
- [6] **Pope A.** – „High-speed wind tunnel testing. John Wiley and Sons Inc”, 1965
- [7] **Ruchała P.**: „Eksperymentalne badania dynamicznych charakterystyk aerodynamicznych profilu ILH-412 M-S w tunelu dużych prędkości N-3”. Sprawozdanie ILot nr 27/BA-A1/09 P, 2009
- [8] **Rowiński R.**: „Warunki techniczne na modele do badań w tunelu N-3. Instrukcja Systemu Jakości ILot nr IK.04/LA, 2004
- [9] **Zwierchanowska B.**: „Kontrolne skrócone badania ciśnieniowe modelu profilu NACA-0012 w tunelu N-3. Raport wewn. ILot nr 26/LA/99/P”, 1999
- [10] **Zwierchanowska B., Kania W.**: „Pressure measurements in N-3 wind tunnel. Procedura wewn. ILot nr JPB.07/LA, 2007
- [11] **Zwierchanowska B., Krzysiak A.**: „Kalibracja tunelu N-3 modelami NACA-0012, ONERA, CAGI”. Sprawozdanie wewn. ILot nr 88/BA/94/D, 1994

Paweł Ruchała

Andrzej Krzysiak

METODYKA NIESTACJONARNYCH BADAŃ PROFILI ŚMIGŁOWCOWYCH

Streszczenie

Praca opisuje metodykę eksperymentalnych niestacjonarnych badań ciśnieniowych, dotyczących śmigłowcowych profili aerodynamicznych. Została ona wdrożona w trakcie badań profilu śmigłowcowego, wykonanych w Zakładzie Aerodynamiki Instytutu Lotnictwa dla PZL Świdnik i Ministerstwa Nauki i Szkolnictwa Wyższego (w ramach projektu celowego „Opracowanie i wdrożenie nowej generacji rozwiązań konstrukcyjnych, technologicznych i materiałowych dla wirnika nośnego i elementów płatowca śmigłowca PZL W-3A Sokół”.

Celem tego typu badań jest modelowanie w warunkach tunelowych zjawiska tzw. przeciągnięcia dynamicznego, które może wystąpić na łopatach wirnika nośnego śmigłowca w czasie lotu postępowego. Powoduje ono silne drgania łopat, wobec czego stanowi istotne ograniczenie osiągnięć śmigłowców.

Zjawisko przeciągnięcia dynamicznego jest związane z szybką zmianą kąta natarcia, jaka występuje w czasie lotu postępowego śmigłowca. Warunki te odwzorowano za pomocą modelu wykonującego ruch oscylujący o zadanej częstotliwości i amplitudzie. Mechanizm wywołujący oscylacje, jak również użyta aparatura pomiarowa, zostały opisane w pracy.

Omawiana metodyka dotyczy badań ciśnieniowych. Opierają się one na wyznaczeniu rozkładów ciśnień na powierzchni przystosowanego do tego modelu.

Ze względu na nierównoczesność pomiarów, na podstawie ich wyników aproksymowano zmianę rozkładu ciśnień w funkcji czasu lub kąta natarcia. Zmianę współczynników siły nośnej i momentu pochylającego wyznaczono przez całkowanie tak wyznaczonego rozkładu ciśnień. Algorytm obliczeń również został omówiony.